Adsorbed Thiophenol and Related Compounds Studied at Pt(111) Electrodes by EELS, Auger Spectroscopy, and Cyclic Voltammetry

Donald A. Stern, Edna Wellner, Ghaleb N. Salaita, Laarni Laguren-Davidson, Frank Lu, Nikola Batina, Douglas G. Frank, Donald C. Zapien, Nicholas Walton, and Arthur T. Hubbard*

Contribution from the University of Cincinnati, Department of Chemistry, Cincinnati, Ohio 45221. *Received September 28, 1987*

Abstract: Adsorption of the following compounds from aqueous solutions at well-defined Pt(111) single-crystal surfaces has been studied: 2,5-dihydroxythiophenol (DHTP); 2,5-dihydroxy-4-methylbenzyl mercaptan (DMBM); thiophenol (TP); pentafluorothiophenol (PFTP); 2,3,5,6-tetrafluorothiophenol (TFTP4); 2,3,4,5-tetrafluorothiophenol (TFTP2); and benzyl mercaptan (BM). Adsorbed layers formed from DHTP or DMBM were found by cyclic voltammetry to undergo reversible two-electron, two-proton electrochemical oxidation–reduction and were shown to be stable under vacuum. Therefore, the results of surface spectroscopy in ultrahigh vacuum are directly applicable to the liquid–solid and vapor–solid chemistry and electrochemistry of these compounds. Packing density (adsorbed moles per unit area) was measured for each compound by quantitative Auger electron spectroscopy. Packing densities of these compounds display a plateau at adsorbate concentration above 1 mM. Vibrational spectra of the adsorbed layers from these compounds were obtained by electron energy-loss spectroscopy (EELS) and were compared with the infrared (IR) spectra of the parent compounds in KBr. The EELS and IR spectra were quite similar except that the mercaptan hydrogen is lost during adsorption, and EELS de-emphasizes the O–H stretching modes of phenolic compound such as DHTP and DMBM. Each of these compounds is evidently attached to Pt(111) predominantly through the sulfur atom. LEED observations reveal that, except for the DMBM layer which has $(2\sqrt{3} \times 2\sqrt{3})R30°$ symmetry, these compounds adsorb without long-range ordering with respect to the Pt(111) surface, although their large, constant packing densty and attachment through the S atom is evidence that the adsorbed molecules are uniformly oriented.

The orientation of aromatic molecules adsorbed from solution onto annealed polycrystalline Pt electrodes has been studied by means of thin-layer electrodes (TLE) as a function of adsorbate molecular structure, adsorbate concentration, nature of the electrolyte and solvent (both aqueous and nonaqueous), chirality, temperature, electrode potential, order of addition of adsorbates, surface roughness, and intermolecular interactions between mixed adsorbates. Reviews have appeared recently.[1-5] Adsorbate orientation was shown to have a profound influence on the course of electrocatalytic oxidaton and reduction.[4]

The present article describes results for nonelectroactive as well as electroactive molecules at well-defined Pt(111) surfaces by use of Auger electron spectroscopy and LEED and employs surface-sensitive vibrational spectroscopy (EELS) to obtain information as to the nature of the adsorbed species and mode of attachment to the surface of a family of compounds related to thiophenol and benzylmercaptan. Along with a series of new compounds, some of the substances previously studied have been examined with the new methods in order to provide points of comparison with the more familiar TLE results. These are the first studies of the subject compounds by means of EELS or Auger spectroscopy. This is also the first time that these compounds have been adsorbed from solution at well-defined electrode surfaces or analyzed at the surface by nonelectrochemical methods.

These experiments demonstrate that the electrochemical properties of adsorbed layers of the subject thiophenols and mercaptans are not altered by lengthy exposure to vacuum. Accordingly, the results of surface spectroscopy in ultrahigh vacuum (UHV) are applicable to the solid–liquid electrochemistry of these and a very large number of similar chemisorbed compounds. Packing density (mol/cm^2) measurements of adsorbed layers by Auger spectroscopy are in excellent agreement with measurements by electrochemical coulometry for compounds amenable to coulometry (2,5-dihydroxythiophenol and 2,5-dihydroxy-4-methylbenzyl mercaptan). The Auger measurements are also in excellent agreement with theoretical packing densities of all the compounds studied based upon covalent and van der Waals radii tabulated by Pauling.[15] Vibrational spectra analogous to far-IR and mid-IR reflection–absorption spectra of the adsorbed layers were obtained at high sensitivity (about 0.01 monolayer) and resolution (80 cm^{-1}) by means of electron energy-loss spectroscopy (EELS). The EELS spectra of these adsorbed layers are sufficiently similar to the IR spectra of the solid compounds that assignment of the EELS spectra can be made by analogy with IR assignments. Specific differences between surface-EELS and solid-IR spectra are useful indications of changes in molecular structure accompanying adsorption. LEED patterns of these adsorbed layers reveal that long-range order is present in the layer only in certain cases, but that the Pt(111) substrate surface remains highly ordered apart from extremely oxidizing (positive) potentials. On the basis of the combined data (Auger, EELS, LEED, electrochemistry) for each compound, structural models are proposed for these adsorbed thiophenols, mercaptans, diphenols, and fluorocarbons. The principal characteristics of adsorbed species displaying reversible electroactivity are also discussed.

Experimental Section

Experimental procedures employed in this work were as described previously.[5] Special vacuum instruments were constructed for these studies such that the electrode surface was characterized by low-energy electron diffraction (LEED), Auger spectroscopy, thermal desorption mass spectrometry (TDMS), and electron energy-loss spectroscopy (EELS) in ultrahigh vacuum (UHV) and by electrochemical methods

(1) Hubbard, A. T.; Stickney, J. L.; Soriaga, M. P.; Chia, V. K. F.; Rosasco, S. D.; Schardt, B. C.; Solomun, T.; Song, D.; White, J. H.; Wieckowski, A. *J. Electroanal. Chem.* **1984**, *168*, 43.

(2) Hubbard, A. T.; Chia, V. K. F.; Frank, D. G.; Katekaru, J. Y.; Rosasco, S. D.; Salaita, G. N.; Schardt, B. C.; Song, D.; Soriaga, M. P.; Stern, D. A.; Stickney, J. L.; White, J. H.; Vieira, K. L.; Wieckowski, A.; Zapien, D. C. In *New Dimensions in Chemical Analysis*; Shapiro, C. L., Ed.; Texas A&M University Press: College Station, Texas, 1985; p 135.

(3) Salaita, G. N.; Lu, F.; Laguren-Davidson, L.; Frank, D. G.; Stern, D. A.; Zapien, D. C.; Batina, N.; Wellner, E.; Walton, N.; Hubbard, A. T. In *Chemically Modified Surfaces*; Leyden, D., Ed.; Gordon and Breach: New York, 1988; Vol. 2.

(4) Hubbard, A. T. In *Comprehensive Chemical Kinetics*; Bamford, C. H., Tipper, D. F. H., Compton, R. G., Eds.; Elsevier: Amsterdam, 1988; Vol. 28, Chapter 1.

(5) Hubbard, A. T. *Chem. Rev.* **1988**, in press.

0002-7863/88/1510-4885$01.50/0

(voltammetry, coulometry) in argon at ambient pressure without intervening contamination. The Pt(111) single-crystal surfaces employed for this work were oriented[6] and polished[7] such that all faces were crystallographically equivalent. All faces were cleaned simultaneously by bombardment with Ar^+ ions at 500 eV and annealed by resistance heating (about 1000 K) in UHV.

Cleaning and annealing were continued until LEED showed an ordered surface and Auger spectroscopy demonstrated that the surface was free of detectable impurities. The clean, ordered Pt(111) surface was isolated in an argon-filled antechamber for immersion into buffered aqueous electrolyte solutions containing the subject adsorbates. Electrode potentials were measured and controlled by means of three-electrode electrochemical circuitry based upon operational amplifiers. The electrochemical cell was constructed of Pyrex glass and Teflon double-wall tubing; spaces between the tubing walls were purged with argon as a necessary measure to prevent diffusion of air through the Teflon tubes transporting the cell atmosphere and electrolyte. The electrochemical cell, equipped with a reference half-cell (Ag/AgCl prepared with 1 M KCl) and a Pt auxiliary electrode, was introduced into the antechamber when needed by means of a bellows assembly and gate valve.

Solutions employed for the adsorption experiments contained 10 mM potassium fluoride (KF, Aesar, Johnson Matthey Inc., Seabrook, NH 03874) adjusted to pH 4 with hydrogen fluoride (HF, Fisher Scientific, Pittsburgh, PA 15219). Solutions for voltammetric/coulometric experiments contained 10 mM trifluoroacetic acid (TFA) as a supporting electrolyte to provide adequate conductivity and pH stabilization. Solutions were prepared from water pyrolytically distilled in pure oxygen through a Pt gauze catalyst (800 °C). Prior to use of such solutions, experiments were performed in which Pt(111) was immersed into the electrolyte followed by evacuation and Auger spectroscopy; the water was found to evaporate without leaving a detectable residue or chemisorbed layer, apart from the electrolyte species themselves.

The subject adsorbates were obtained from the following sources and were used as received: thiophenol (TP), pentafluorothiophenol (PFTP),

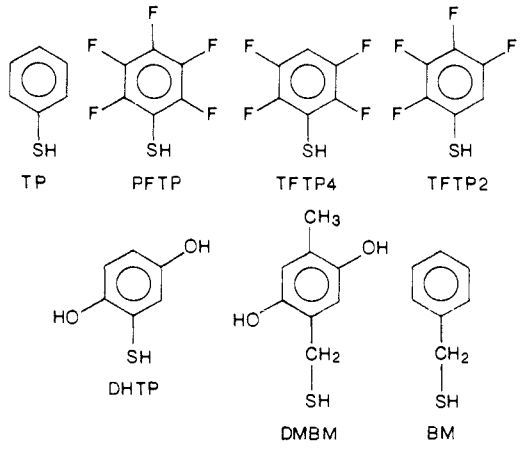

2,3,5,6-tetrafluorothiophenol (TFTP4), and trifluoroacetic acid (TFA) from Aldrich Chemical Co. (Milwaukee, WI 53201); 3,4,5,6-tetrafluorothiophenol (TFTP2) from Columbia Organic Chemical Co. (Camden, SC 29020). Dihydroxythiophenol (DHTP) was synthesized according to published procedures;[8] and we are grateful to D. L. Fields for providing us with a sample of pure 2,5-dihydroxy-4-methylbenzyl mercaptan (DMBM).[9]

Packing densities, expressed as F_x (moles of element x adsorbed per cm^2) or as F (molecular packing density, mol/cm^2), were measured by two independent methods (see ref 11 for details):

(i) The Auger signal at 235 eV due to the Pt substrate was measured before (I_{Pt}^0) and after (I_{Pt}) formation of the adsorbed layer. In order to minimize the influence of overlap between the Pt signal and that due to C the positive-going half of the derivative spectrum was used as a measure of the Pt peak height. The substrate signal ratio I_{Pt}/I_{Pt}^0 was converted to packing density by means of an equation of the following form

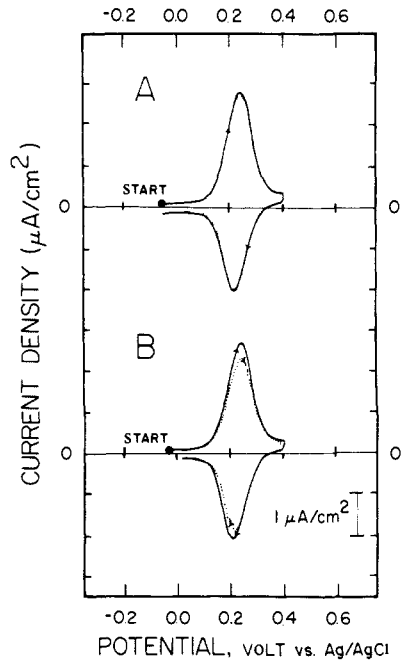

Figure 1. Cyclic voltammetry of adsorbed DMBM at Pt(111). (A) Solid curve (—): immersion into 0.7 mM DMBM followed by rinsing with 10 mM TFA. Dotted curve (···): as above followed by 1 h under vacuum prior to voltammetry. (b) Solid curve (—): first scan. Dotted curve (···): second scan. Scan rate: 5 mV/s.

$$I_{Pt}/I_{Pt}^0 = \prod_{i=1}^{N}(1 - J_i K_x \Gamma) \quad (1)$$

where J_i represents the number of non-hydrogen atoms per molecule located in the ith level of the adsorbed layer, and N is the outermost layer. Auger spectral data collected for a variety of compounds have revealed that K_x for the Pt signal at 235 eV is equal to 0.153 $cm^2/nmol$ for light elements such as C, N, and O. The magnitude of K_x for sulfur atoms is K_S = 0.219 $cm^2/nmol$, based upon Auger spectra and voltammetric data for DMBM at Pt(111) in the plateau region of packing density. This approach to determination of Γ based upon measurement of substrate Auger signal and use of electron-scattering formulas has the advantage that the results are independent of spectrometer characteristics and require only that the spectra be reproducible. Conversion of elemental packing densities, Γ_x, to molecular packing densities, Γ, was based upon molecular formulas. Hydrogen atoms were averaged in with the other elements and were not treated separately. The results of application of eq 1 were in excellent agreement with determinations based upon measurement of elemental Auger signals.[11] Packing density is also conveniently expressed in atoms per surface Pt atom

$$\Theta = \Gamma/\Gamma_{Pt} \quad (2)$$

where Γ_{Pt} = 1.50 × 10^{15} atoms/cm^2 for Pt(111).

(ii) Auger signals, I_x, due to each element x were measured, from which the packing densities, Γ_x, were calculated

$$\Gamma_x = (I_x/I_{Pt}^0)/(B_x \sum_{i=1}^{N} L_i a_i) \quad (3)$$

where B_x is a proportionally coefficient appropriate to element x, L_i is the fraction of element x atoms in level i (i = 1 is closest to the surface), and a_i is the scattering factor for Auger electrons emitted from the ith atom of element x in the layer: $a_i = (f_x)^{M_i}$, where M_i is the number of atoms located on the path from the emitting atom to the detector. Specifics of these equations are summarized in Table IV.

Electron energy-loss spectra (EELS) were obtained by means of a Kesmodel EELS spectrometer (Bloomington, IN 47405). The beam incident on the sample was approximately 0.1 nA and 4 eV. The spectrometer was operated at a resolution of about 10 meV (80 cm^{-1}) in these experiments.

Infrared spectra of solutions and solid compounds were obtained with a Perkin-Elmer Model 1420 dispersive instrument operated at 4-cm^{-1}

(6) Wood, E. A. *Crystal Orientation Manual*; Columbia University Press: New York, 1963.
(7) Samuels, L. E. *Metallographic Polishing by Mechanical Methods*; Pittman: London, 1963.
(8) Alcalay, W. *Helv. Chim. Acta* **1947**, *30*, 578.
(9) Fields, D. L.; Miller, J. B.; Reynolds, D. D. *J. Org. Chem.* **1965**, *30*, 3962.
(10) (a) Schoeffel, J. A.; Hubbard, A. T. *Anal. Chem.* **1977**, *49*, 2330. (b) Garwood, G. A., Jr.; Hubbard, A. T. *Surf. Sci.* **1982**, *118*, 223. (c) Katekaru, J. Y.; Hershberger, J.; Garwood, G. A., Jr.; Hubbard, A. T. *Surf. Sci.* **1982**, *121*, 396. (d) Chia, V. K. F.; Stickney, J. L.; Soriaga, M. P.; Rosasco. S. D.; Salaita, G. N.; Hubbard, A. T.; Benziger, J. B.; Pang, K. W. P. *J. Electroanal. Chem.* **1984**, *163*, 407.
(11) Lu, F.; Salaita, G. N.; Laguren-Davidson, L.; Stern, D. A.; Wellner, E.; Frank, D. G.; Batina, N.; Walton, N.; Hubbard, A. T. *Langmuir*, in press.

Table I. Auger Spectroscopic Data and Electrochemical Data[a]

	normalized Auger peak heights					coulometric charge density
−log C	I_C/I_{Pt}^0	I_O/I_{Pt}^0	I_{Pt}/I_{Pt}^0	I_S/I_{Pt}^0	I_F/I_{Pt}^0	$(Q - Q_b)/A$, $\mu C/cm^2$
			2,5-Dihydroxy-4-methylbenzyl Mercaptan (DMBM)			
6.00	0.087	0.116	0.843	0.884		19.7
5.52	1.225	0.366	0.749	3.495		22.5
5.00	1.341	0.400	0.676	4.606		45.6
4.52	2.039	0.469	0.500	4.161		63.7
4.00	1.961	0.510	0.490	3.772		70.6
3.52	2.251	0.606	0.481	4.760		71.7
3.16	2.117	0.541	0.455	3.996		73.4
			2,5-Dihydroxythiophenol (DHTP)			
3.16	0.977	0.333	0.625	3.630		50.8
			Thiophenol (TP)			
4.0	1.743		0.645	2.560		
			Pentafluorothiophenol (PFTP)			
4.0	2.070		0.639	2.172	0.374	
			Benzyl Mercaptan (BM)			
4.0	1.946		0.635	3.454		
			2,3,5,6-Tetrafluorothiophenol (TFTP4)			
4.0	1.938		0.626	1.708	0.239	
			2,3,4,5-Tetrafluorothiophenol (TFTP2)			
4.0	1.342		0.667	1.638	0.390	

[a] Experimental conditions: Adsorbate concentration, C, is expressed in mol/L; the electron beam was 0.1 μA at 2000 eV, incident normal to the Pt(111) surface. Modulation amplitude at the cylindrical mirror was 5 V peak-to-peak; Auger peak heights were normalized by the height of the positive lobe of the Pt Auger signal at 235 eV; supporting electrolyte was 10 mM KF adjusted to pH 4 with HF; electrode potential was 0.2 V vs Ag/AgCl (1 M KCl) reference.

Table II. Packing Densities of Thiophenols and Related Compounds

	packing densities from elemental Auger signals					packing density from Pt Auger signal attenuation,	packing density from coulometry
−log C	Γ_C, nmol/cm^2	Γ_O, nmol/cm^2	Γ_S, nmol/cm^2	Γ_F, nmol/cm^2	Γ, nmol/cm^2	Γ, nmol/cm^2	$(Q - Q_b)/2FA$, Γ_{el}, nmol/cm^2
			2,5-Dihydroxy-4-methylbenzyl Mercaptan (DMBM)				
6.00	0.123	0.123	0.08		0.015	0.094	0.102
5.52	1.725	0.379	0.30		0.216	0.156	0.117
5.00	1.889	0.414	0.40		0.236	0.207	0.237
4.52	2.872	0.486	0.36		0.359	0.344	0.331
4.00	2.762	0.528	0.33		0.345	0.354	0.366
3.52	3.170	0.627	0.41		0.396	0.362	0.371
3.16	2.982	0.560	0.35		0.373	0.386	0.381
			2,5-Dihydroxythiophenol (DHTP)				
3.16	1.556	0.314	0.39		0.259	0.298	0.261
			Thiophenol (TP)				
4.0	2.686		0.27		0.448	0.356	
			Pentafluorothiophenol (PFTP)				
4.0	3.296		0.23	2.03	0.549	0.218	
			Benzyl Mercaptan				
4.0	2.295		0.30		0.328	0.299	
			2,3,5,6-Tetrafluorothiophenol (TFTP4)				
4.0	3.198		0.183	1.34	0.533	0.244	
			2,3,4,5-Tetrafluorothiophenol (TFTP2)				
4.0	2.261		0.175	2.05	0.377	0.216	

resolution. Reference IR spectra were obtained from published sources whenever possible.[12]

Results and Discussions

(1) 2,5-Dihydroxy-4-methylbenzyl Mercaptan (DMBM). Shown in Figure 1A (solid curve) is the cyclic voltammogram obtained with a Pt(111) surface which had been immersed into 0.5 mM 2,5-dihydroxy-4-methylbenzyl mercaptan (DMBM) followed by rinsing with pure supporting electrolyte at 0.2 V (vs Ag/AgCl, 1 M KCl reference). Clearly, DMBM forms an adsorbed layer on the Pt(111) surface which does not rinse away, and which displays a reversible electrode reaction. Shown for comparison in Figure 1A (dotted curve) is the cyclic voltammogram obtained when (in addition to adsorption of DMBM and rinsing in electrolyte) the surface was evacuated to UHV for about 1 h (during which EELS and Auger spectra were obtained) *prior to* the voltammetry. *As can be seen, the two results are essentially identical, indicating that the adsorbed layer formed from DMBM is retained quantitatively at the surface under vacuum. On the other hand, cyclic voltammetry causes appreciable damage to the layer, as can be seen from a comparison of the first and second voltammetric cycles, Figure 1B.*

(12) (a) Pouchert, C. J. *The Aldrich Library of FTIR Spectra*; Aldrich Chemical Co., Inc.; Milwaukee, 1985. (b) *Standard Spectra Collection*; Sadtler Research Laboratories, Inc.: Philadelphia, PA, 1980.

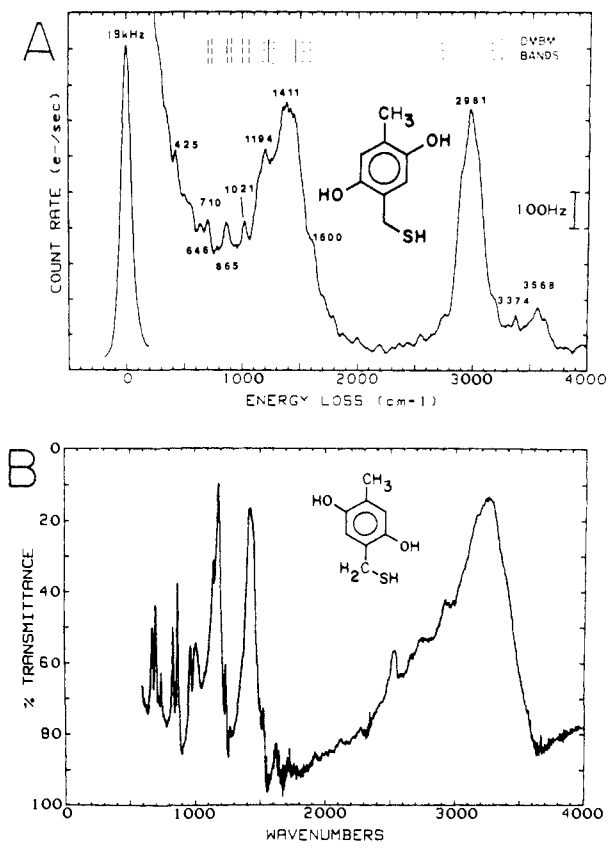

Figure 2. Vibrational spectra of DMBM. (A) EELS spectrum of adsorbed DMBM at Pt(111). The locations of the mid-IR absorption bands are also shown: (···) weak, (- - -) strong, (—) very strong. (B) IR spectrum of solid DMBM in KBr. Experimental conditions: DMBM solution concentration, 0.1 mM in 10 mM KF/HF electrolyte (pH 4); EELS incidence and detection angles, 62° from surface normal; beam energy, 4 eV; beam current 0.15 nA; EELS resolution, 10 meV (80 cm^{-1}) fwhm; IR resolution, 4 cm^{-1} fwhm.

The electron energy-loss spectrum (EELS) of DMBM adsorbed at Pt(111) is shown in Figure 2A. Also shown is the infrared spectrum of solid DMBM in KBr, Figure 2B. Only the mid-IR spectrum is shown (600–4000 cm^{-1}). There is a high degree of correspondence between the EELS spectrum of adsorbed DMBM and the IR spectrum of solid DMBM, except that the S–H stretch (2500 cm^{-1}) is absent from the EELS spectrum. Proposed assignments of the EELS bands have been made with reference to the accepted IR assignments of the parent compounds and are given in Table III. Although the S–H band is not particularly intense in the IR spectrum of solid DMBM, the absence of an S–H band in the EELS spectrum is evidence for removal of the mercaptan hydrogen during the adsorption reaction: The adsorbed diphenol is stable in contact with solution, as evidenced by the stability of the electrode potential at open circuit. Furthermore, when the layer was removed from solution, evacuated to UHV for about 1 h, then transferred back into solution from vacuum, the open-circuit electrode potential was about the same as before evacuation; and, when the potential was scanned in the positive direction, the usual peak indicative of the adsorbed diphenol was observed, Figure 1A.

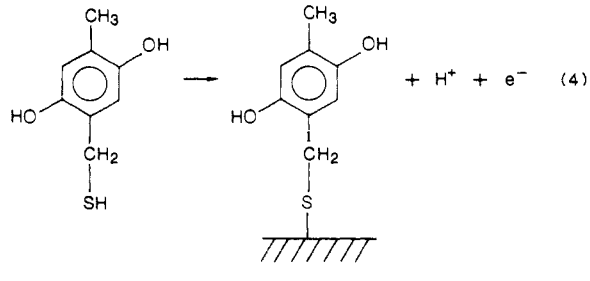

Table III. Assignments of EELS Bands of Adsorbed Thiophenols

compd[a]	freq, cm^{-1}	symmetry species	description
DMBM	3568	C_1: A	OH stretch(meta)
	3374		OH stretch(ortho)
	2981		CH stretch
	1600		CC stretch
	1411		CC stretch
	1194		CO stretch
	1021		CH bend
	865		CH bend
	710		ring bend
	646		CS stretch
	425		ring bend
DHTP	3508	C_s: A′	OH stretches
	3048	A′	CH stretch
	1574	A′	CC stretch
	1463	A′	CC stretch
	1171	A′	CO stretch
	821	A″	CH bend
	821	A′	ring bend
	409	A″	ring bend
	290	A′	PtS stretch
TP	3057	C_{2v}: A_1, B_2	CH stretches
	1516	A_1, B_2	CC stretches
	1428	A_1, B_2	CC stretches
	1145	B_2	CH bend
	726	B_1	CH bend
	395	B_2	ring bend
PFTP	1632	C_{2v}: A_1, B_2	CC stretches
	1532	A_1, B_2	CC stretches
	1103	A_1, B_2	CF stretches
	802	B_2	CF bend
	600	B_1	CF bend, CS stretch
	330	A_1	PtS stretch
BM	3042	C_{2v}: A_1, B_2	CH stretches
	1600	A_1, B_2	CC stretches(ring)
	1477	A_1, B_2	CC stretches
	1166	B_2	CH bend(ring)
	1000	A_1	CH bend(CH_2)
	736	B_1	CH bend(ring)
	400	B_2	ring bend
TFTP4	3092	C_{2v}: A_1	CH stretch
	1599	A_1, B_2	CC stretches
	1427	A_1, B_2	CC stretches
	1207	B_2	CH bend
	1040	A_1, B_1	CF stretches
	832	B_2	CF bend
	703	A_1	CS stretch
	496	B_1	CF bend
	313	A_1	PtS stretch
TFTP2	3000	C_s: A′	CH stretch
	1600	A′, A″	CC stretches
	1490	A′, A″	CC stretches
	1234	A″	CH bend
	1097	A′, A″	CF stretches
	778	A′	CF bend
	700	A'	CS stretch
	447	A''	CF bend
	300	A′	PtS stretch

[a] DMBM = 2,5-dihydroxy-4-methylbenzyl mercaptan. DHTP = 2,5-dihydroxythiophenol. TP = thiophenol. PFTP = pentafluorothiophenol. BM = benzyl mercaptan. TFTP4 = 2,3,5,6-tetrafluorothiophenol. TFTP2 = 2,3,4,5-tetrafluorothiophenol.

The Auger spectrum following adsorption of DMBM at Pt(111) is shown in Figure 3B. Auger data and packing densities are given in Figures 3 and 4 and Tables I and II. Packing densities were obtained from C, O, and S Auger signals by means of eq 5–7 in Table IV, where I_{Pt} was measured at the positive lobe of the Pt signal at 235 eV to minimize the effect of overlap with other peaks in the spectrum.

The limiting molecular packing density, Γ, from Γ_C is $\Gamma_C/8$ = 0.373 nmol/cm^2. Molecular packing density was also determined from attenuation of the Pt Auger signal (positive lobe at 235 eV), eq 8 in Table IV. The result is Γ = 0.386 nmol/cm^2. The theoretical molecular packing density from covalent and van der Waals radii[15] for the proposed structure shown in Figure 5C is 0.399 nmol/cm^2 (41.7 $Å^2$/molecule).

Table IV. Formulas for Obtaining Packing Density from Auger Spectra

compd	formula[a]	eq no.
DMBM	$\Gamma_C = (I_C/I_{Pt}^0)/[B_C(1/2 + 7f_C^2/16)]$	(5)
	$\Gamma_O = (I_O/I_{Pt}^0)/[B_O(1/2 + f_O/4 + f_O^3/4)]$	(6)
	$\Gamma_S = (I_S/I_{Pt}^0)/(B_S f_S)$	(7)
	$I_{Pt}/I_{Pt}^0 = (1 - K_S\Gamma)(1 - 5K_C\Gamma)^2$	(8)
DHTP	$I_{Pt}/I_{Pt}^0 = (1 - K_X\Gamma)(1 - 4K_C\Gamma)^2$	(13)
	$\Gamma_C = (I_C/I_{Pt}^0)/[B_C(1/4 + 7f_C/12 + f_C^2/6)]$	(14)
	$\Gamma_O = (I_O/I_{Pt}^0)/[B_O(3/4 = F_O^3/4)]$	(15)
	$\Gamma_S = (I_S/I_{Pt}^0)/[B_S(f_S/2 + f_S^2/2)]$	(16)
TP	$I_{Pt}/I_{Pt}^0 = (1 - K_S\Gamma)(1 - 3K_C\Gamma)^2$	(19)
	$\Gamma_C = (I_C/I_{Pt}^0)/[B_C(1/3 + f_C/2 + f_C^2/6)]$	(20)
	$\Gamma_S = (I_S/I_{Pt}^0)/[B_S(f_S/2)]$	(21)
PFTP	$\Gamma_{Pt}/I_{Pt}^0 = (1 - K_S\Gamma)(1 - 5K_C\Gamma)^2(1 - K_C\Gamma)$	(22)
	$\Gamma_C = (I_C/I_{Pt}^0)/[B_C(1/4 + 7f_C/12 + f_C^2/6)]$	(23)
	$\Gamma_F = (I_F/I_{Pt}^0)[B_F(4/5 + f_F^2/5)]$	(24)
	$\Gamma_S = (I_S/I_{Pt}^0)/[B_S(f_S/2 + f_S^2/2)]$	(25)
BM	$I_{Pt}/I_{Pt}^0 = (1 - K_S\Gamma)(1 - 7K_C\Gamma)$	(26)
	$\Gamma_C + (I_C/I_{Pt}^0)/B_C$	(27)
	$\Gamma_S = (I_S/I_{Pt}^0)/(B_S f_S)$	(28)
TFTP4	$I_{Pt}/I_{Pt}^0 = (1 - K_S\Gamma)(1 - 5K_C\Gamma)^2$	(29)
	$\Gamma_C = (I_C/I_{Pt}^0)/[B_C(1/6 + 2f_C/3 + f_C^2/6)]$	(30)
	$\Gamma_F = (I_F/I_{Pt}^0)/[B_F(3/4 + f_F^2/4)]$	(31)
	$\Gamma_S = (I_S/I_{Pt}^0)/[B_S(f_S/2 + f_S^2/2)]$	(32)
TFTP2	$I_{Pt}/I_{Pt}^0 = (1 - K_S\Gamma)(1 - K_C\Gamma)(1 - 4K_C\Gamma)(1 - 5K_C\Gamma)$	(33)
	$\Gamma_C = (I_C/I_{Pt}^0)/(B_C f_C)$	(34)
	$\Gamma_F = I_F/I_{Pt}^0)/[B_F(3/4 + f_F^3/4)]$	(35)

[a] Constants: $B_C = 0.848$ cm²/nmol; $B_O = 1.27$ cm²/nmol; $B_S = 18.6$ cm²/nmol; $B_F = 0.205$ cm²/nmol. $f_C = f_O = f_F = 0.70$; $f_S = 0.62$.

Integration of the voltammetric current for reversible oxidation of DMBM chemisorbed at 0.7 mM yielded a coulometric charge for oxidation of the adsorbed species, $(Q - Q_b) = 7.34 \times 10^{-5}$ C/cm². [Background charge, Q_b, was compensated approximately by linear interpolation between the starting point and the small current at the tail of the peak.] On the basis of this result and the Faraday law, eq 9, with $n = 2$, the, molecular packing density

$$\Gamma_{el} = (Q - Q_b)/(nFA) \tag{9}$$

is $\Gamma_{el} = 0.381$ nmol/cm². The values found by Auger spectroscopy, eq 5 and 8, are $\Gamma = 0.373$ and 0.386 nmol/cm². The similarity of Γ values obtained by coulometry and Auger spectroscopy indicates that essentially all of the chemisorbed molecules are electroactive. The voltammetric peak potential for the adsorbed layer (0.26 V vs Ag/AgCl reference at pH 2) was the same as the equilibrium potential of unadsorbed DMBM (0.26 V) and varied with pH in the expected manner,[13] Comparison of the packing density deduced from Auger data with the coulometric data (Table I) suggests that the electrode reaction is

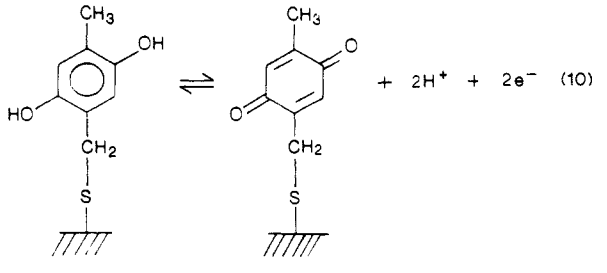

Allowing, as usual, for the contribution due to background reactions, the current follows the thin-layer voltammetric equation,[14] except for introduction of a parameter to compensate for surface intermolecular redox interactions:[13]

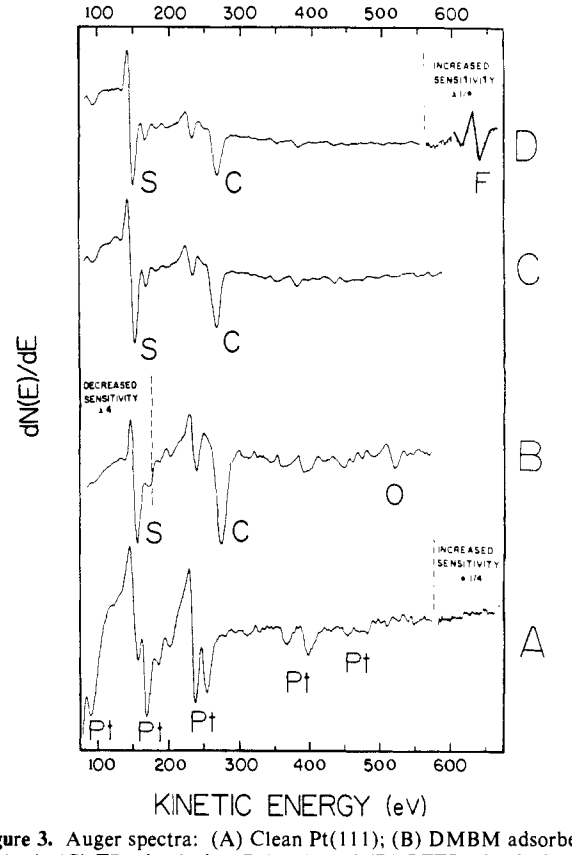

Figure 3. Auger spectra: (A) Clean Pt(111); (B) DMBM adsorbed at Pt(111); (C) TP adsorbed at Pt(111); and (D) PFTP adsorbed on Pt-(111). Experimental conditions: adsorbate concentrations, 0.7 mM; beam at normal incidence, 100 nA, 2000 eV.

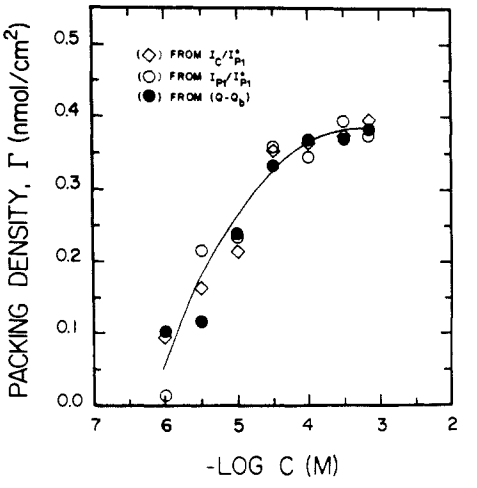

Figure 4. Packing density of DMBM at Pt(111) based upon I_{Pt}/I_{Pt} (◇), eq 8; I_C/I_{Pt}^0 (○), eq 5; and cyclic voltammetry (●), eq 9. Experimental conditions: 10 mM KF/HF (pH 4) electrolyte; temperature, 23 ± 1 °C; electrode potential, 0.20 V vs Ag/AgCl (1 M KCl) reference; scan rate, 5 mV/s.

$$i = \frac{\gamma n^2F^2A\Gamma(-r)\exp\left[\dfrac{\gamma nF}{RT}(E - E^0)\right]}{RT\left\{1 + \exp\left[\dfrac{\gamma nF}{RT}(E - E^0)\right]\right\}^2} \tag{11}$$

where $\Gamma = 0.37$, r is the scan rate, and the other symbols have their usual meanings. The observed broadening of the current–potential curves (reflected by the parameter γ) for adsorbed

(13) (a) Soriaga, M. P.; Hubbard, A. T. *J. Am. Chem. Soc.* **1982**, *104*, 3397. (b) Soriaga, M. P.; Hubbard, A. T. *J. Electroanal. Chem.* **1983**, *159*, 101.

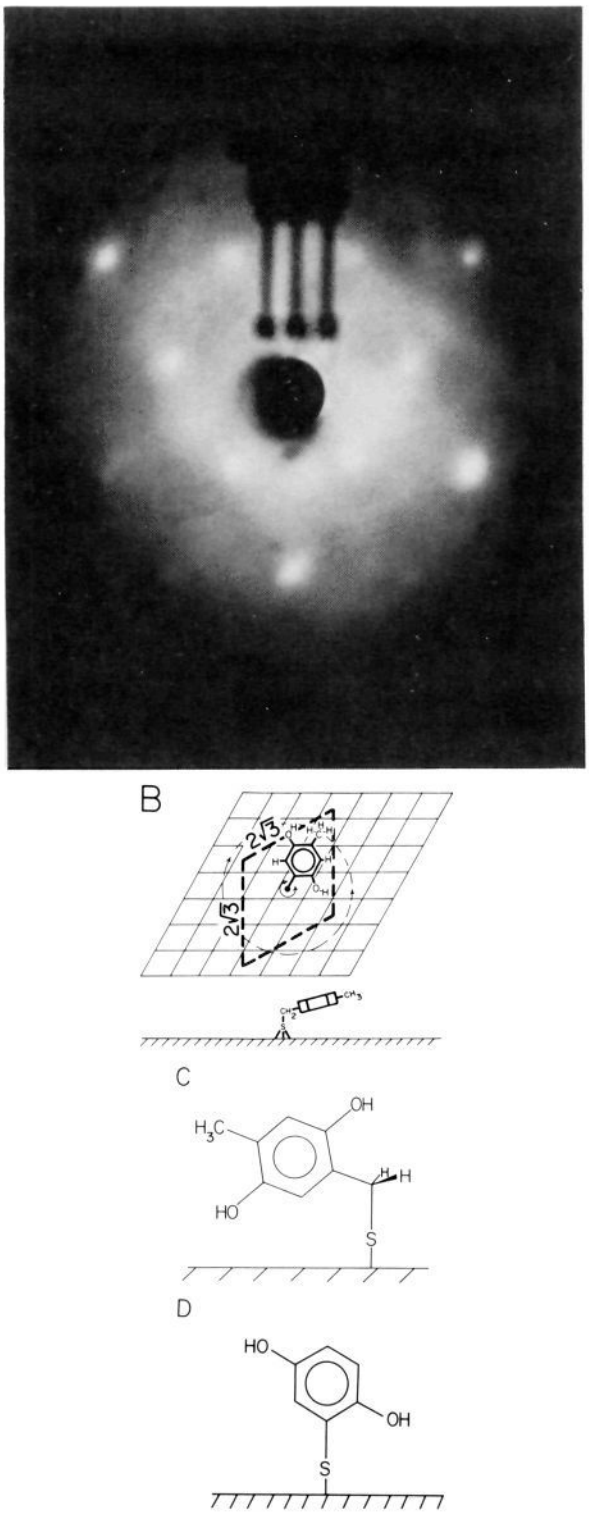

Figure 5. LEED pattern and structural models of species adsorbed at Pt(111). (A) Pt(111)($2\sqrt{3} \times 2\sqrt{3}$)$R30°$ LEED pattern of adsorbed DMBM at $\Gamma = 0.2$ nmol/cm^2. (B) DMBM structural model, Γ(theor) = 0.208 nmol/cm^2. (C) DMBM structural model, Γ(theor) = 0.399 nmol/cm^2. (D) DHTP structural model, Γ(theor) = 0.572 nmol/cm^2. Experimental conditions: LEED beam energy, 70 eV; electrolyte, 10 mM KF/HF (pH = 4); electrode potential, 0.2 V vs Ag/AgCl (1 M) reference; DMBM concentration, 0.01 mM.

DMBM and related compounds relative to the current–potental curves of the unadsorbed compounds is probably due to electronic interactions between adsorbed molecules and the Pt surface, somewhat analogous to the interaction of multiple redox or acidic/basic centers within a molecule.

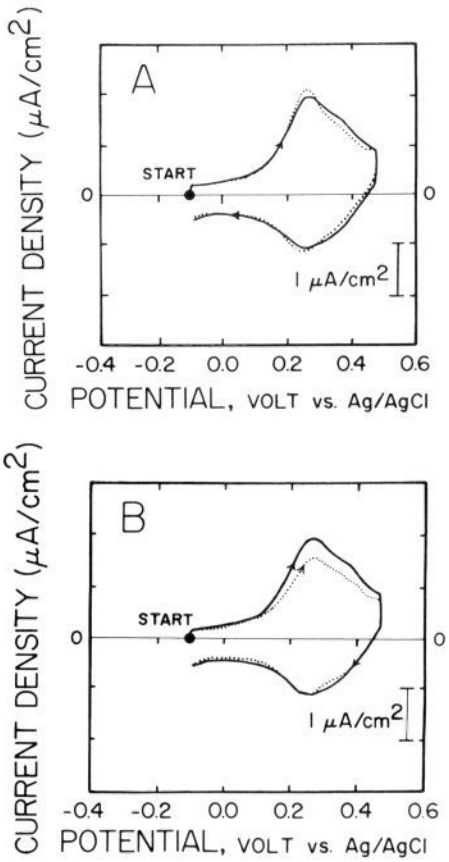

Figure 6. Cyclic voltammetry of adsorbed DHTP at Pt(111). (A) Solid curve (—): immersion into 0.7 mM DHTP followed by rinsing with 10 mM TFA. Dotted curve (···): as above, but with 1 h under vacuum prior to voltammetry. (B) Solid curve (—): first scan. Dotted curve (···): second scan. Scan rate: 5 mV/s.

LEED patterns for DMBM adsorbed from 0.01 mM DMBM solution displayed beams characteristic of ($2\sqrt{3} \times 2\sqrt{3}$)$R30°$ symmetry, Figure 5A. The 2/6-index beams were much more distinct than the 1/6-index beams, indicating that a repeat distance resembling that in ($\sqrt{3} \times \sqrt{3}$)$R30°$ structures occurs frequently in the structure. The packing density of DMBM in this structure, $\Gamma = 0.236$, 0.207, or 0.237 nmol/cm^2, Table II, is close to that expected for a $2\sqrt{3}$ structure, $\theta = 1/12$, or $\Gamma = 0.208$ nmol/cm^2. Since the packing density of DMBM in this ordered structure is much less than the maximum observed packing density, $\Gamma = 0.4$ nmol/cm^2, the DMBM molecules are evidently shared in some way among the neighboring spaces in order to span the $2\sqrt{3}$ unit mesh. Figure 5B illustrates one way in which this could occur: rotation of the benzylic moiety around the C–S bond should be facile, allowing the benzyl pendant to sweep through the entire area of a $2\sqrt{3}$ cell. When pointing toward each other, adjacent pendants are a distance of about $\sqrt{3}$ apart.

(2) 2,5-Dihydroxythiophenol (DHTP). Comparing the behavior of DMBM to the closely related compound 2,5-dihydroxythiophenol (DHTP) proves to be informative. The cyclic voltammogram of chemisorbed DHTP is shown in Figure 6A. As expected, DHTP forms a chemisorbed layer on the Pt(111) surface which does not rinse away and which displays a reversible electrode reaction (solid curve). The dotted curve was obtained when (in addition to adsorption of DHTP and rinsing with pure electrolyte) the surface was evacuated to UHV for about 1 h prior to voltammetry. As can be seen, the two results are essentially identical,

(14) (a) Hubbard, A. T.; Anson, F. C. *Anal. Chem.* **1966**, *38*, 58. (b) Hubbard, A. T. *J. Electroanal. Chem.* **1969**, *22*, 165. (c) Hubbard, A. T. Ph.D. Thesis, California Institute of Technology, 1967 (University Microfilms, Ann Arbor, Michigan, document No. 67-6006).

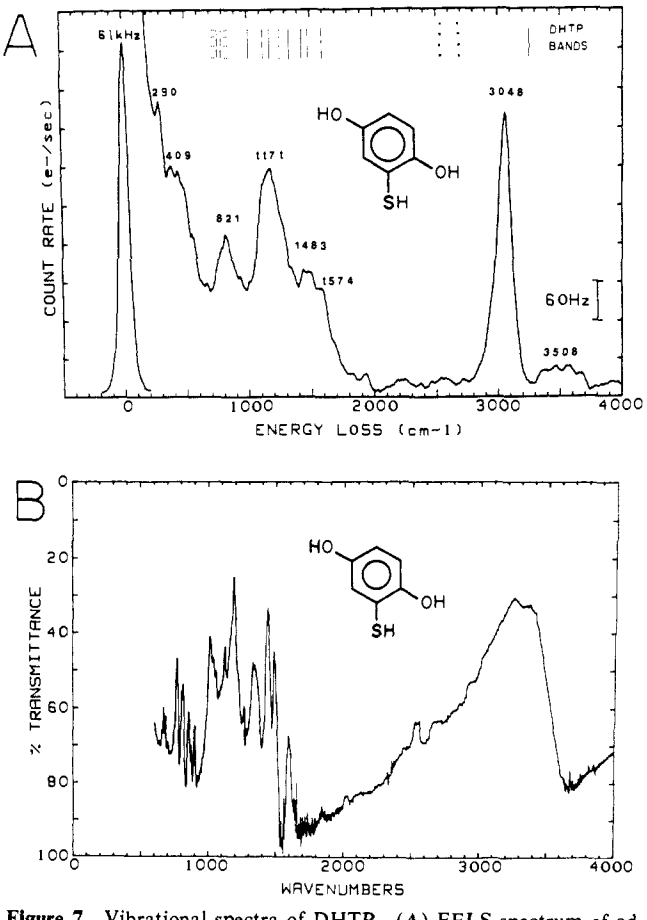

Figure 7. Vibrational spectra of DHTP. (A) EELS spectrum of adsorbed DHTP at Pt(111). (b) IR spectrum of solid DHTP (KBr pellet). Experimental conditions: DHTP solution concentration, 0.5 mM; other conditions as in Figure 2.

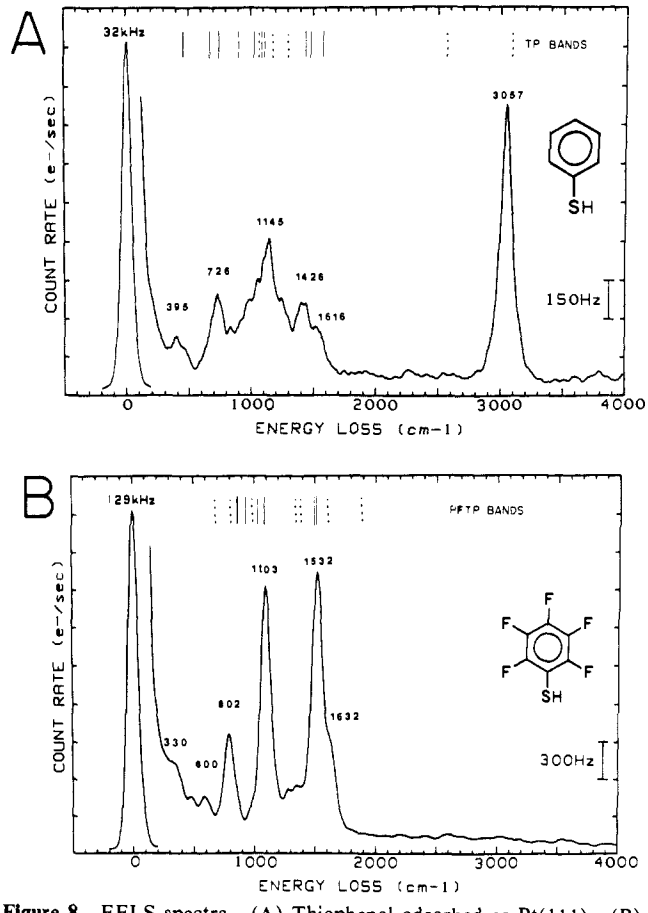

Figure 8. EELS spectra. (A) Thiophenol adsorbed as Pt(111). (B) Pentafluorothiophenol adsorbed at Pt(111). Experimental conditions as in Figure 2.

indicating that the adsorbed layer formed from DHTP is stable under vacuum. However, cyclic voltammetry causes appreciable damage to the layer, as can be seen from a comparison of the first and second voltammetric cycles, Figure 6B.

Voltammograms of DHTP are broadened to an even greater extent ($\gamma = 0.31$ in eq 11) than those for DMBM ($\gamma = 0.37$). Apparently, the benzyl methylene carbon isolates the electroactive ring from the surface more completely than the mercaptan alone, as discussed in ref 13.

Additional clues are provided by the EELS spectrum of Pt(111) after treatment with DHTP, Figure 7A, and the mid-IR spectrum of solid DHTP (KBr pellet), Figure 7B. As expected, the EELS spectrum of the adsorbed layer bears a striking resemblance to the IR spectrum of solid DHTP, except that the S–H stretch (2500 cm^{-1}) and the S–H bend (1020 cm^{-1}) are absent from the EELS spectrum. Once again, this suggests that loss of the mercaptan hydrogen accompanies adsorption:

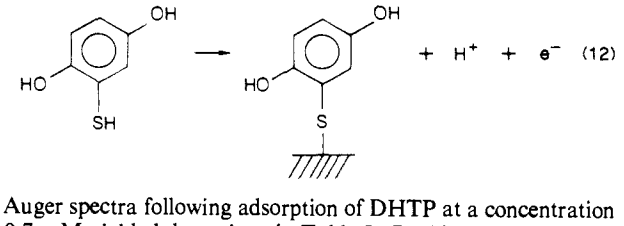

Auger spectra following adsorption of DHTP at a concentration of 0.7 mM yielded data given in Table I. Packing densities were calculated by means of eq 13–16 in Table IV. The molecular packing density obtained from the carbon Auger signal by use of eq 14, $\Gamma = 0.259$ nmol/cm^2, is unexpectedly small (the theoretical value is 0.572 nmol/cm^2, 29.01 Å^2/molecule), and is smaller than the result obtained from attenuation of the Pt Auger signal (eq 13), $\Gamma = 0.298$ nmol/cm^2. The molecular packing density obtained from reversible coulometric data was also unexpectedly

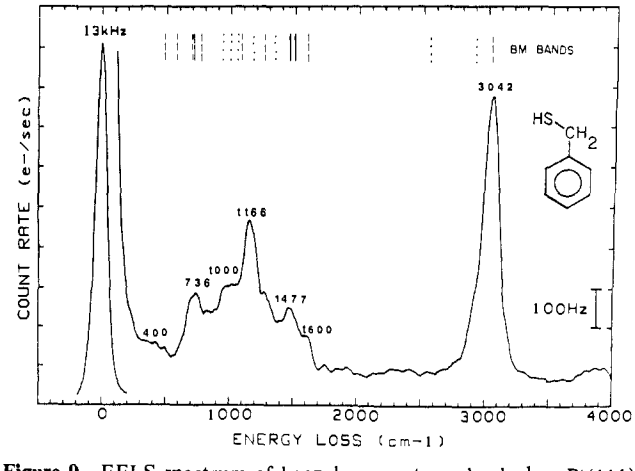

Figure 9. EELS spectrum of benzyl mercaptan adsorbed at Pt(111). Experimental conditions as in Figure 2.

small, $\Gamma_{el} = 0.261$ nmol/cm^2, and was essentially identical with the carbon Auger result. The elemental ratios were also unexpected: C/S = 2.1 compared with the expected value (6.0) and O/S = 0.42 compared with the expected value (2.0). The most likely explanation is that chemisorption of DHTP is accompanied by spontaneous elimination of the *p*-diphenol moiety from about 50% of the adsorbed material:

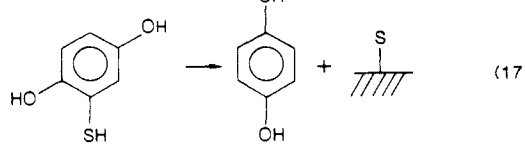

In fact, efficient reductive elimination of the pendent hydroquinone

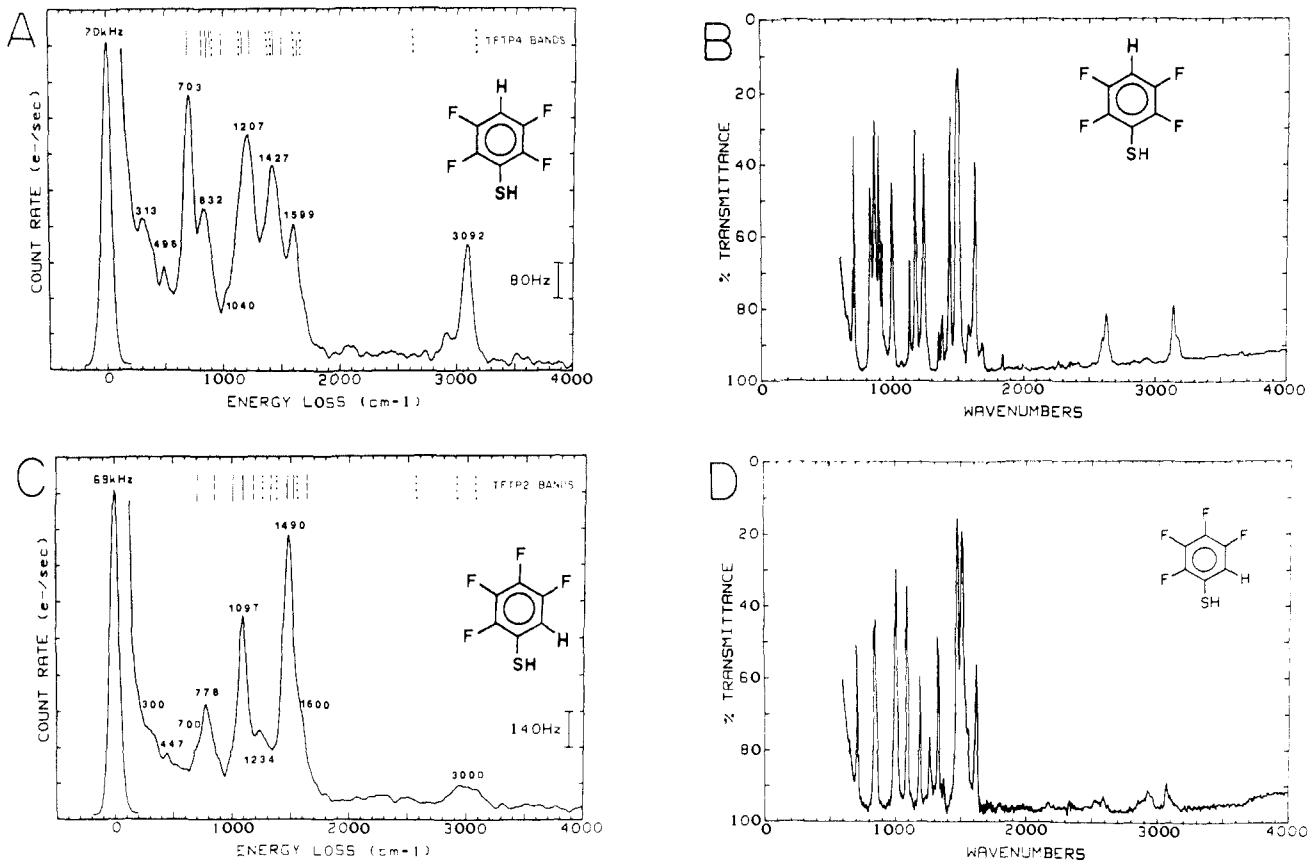

Figure 10. Vibrational spectra. (A) EELS spectrum of 2,3,5,6-tetrafluorothiophenol (TFTP4) adsorbed at Pt(111). (b) IR spectrum of TFTP4 (neat liquid). (c) EELS spectrum of 2,3,4,5-tetrafluorothiophenol (TFTP2) adsorbed at Pt(111). (D) IR spectrum of TFTP2 (neat liquid). Experimental conditions as in Figure 2.

moiety was found earlier (4e) by means of capillary gas chromatography combined with thin-layer electrochemistry.

(3) Thiophenol (TP). The EELS spectrum of the parent compound in this series, thiophenol (TP), is shown in Figure 8A. Also shown are the locations of principal mid-IR infrared bands of TP. As expected from the results for DMBM, DHTP, BM, and TP, the EELS spectrum of the adsorbed layer correlates closely with the IR spectrum of the solid sample, except that the S–H band of TP (2567 cm^{-1}) is weak or absent from the EELS spectrum of adsorbed TP:

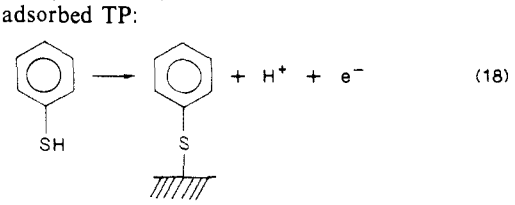

(18)

There is also the expected close resemblance between the EELS spectrum of TP and those of related compounds in Figures 2, 6, 8, and 9. Auger data for TP, Figure 3C and Tables I and II, are consistent with the results for the related compounds. Packing densities were obtained by means of eq 19–21 in Table IV. The molecular packing density from Pt signal attenuation, $\Gamma = 0.36$ nmol/cm^2, and from the carbon Auger signal, $\Gamma = 0.45$ nmol/cm^2, was considerably smaller than the theoretical limiting value,[15] 0.670 nmol/cm^2 (24.8 $Å^2$). This is probably a result of the virtual insolubility of TP in water, leading to very low adsorbate concentration and limited packing density.

(4) Pentafluorothiophenol (PFTP). Comparison of EELS spectra obtained for adsorbed TP, Figure 8A, and for adsorbed pentafluorothiophenol (PFTP), Figure 8B, is of interest because PFTP contains no C–H bonds. Appropriately, the C–H stretching band is absent from the EELS spectrum of PFTP, Figure 8B.

(15) Pauling, L. C. *The Nature of the Chemical Bond*, 3rd ed.; Cornell University Press: Ithaca, NY, 1960.

Packing densities were calculated from Auger data by means of eq 22–25 in Table IV where $B_F = 0.205$ and $f_F = 0.7$. The molecular packing density from Pt Auger signal attenuation was 0.22 nmol/cm^2, and from the carbon Auger signal it was 0.55 nmol/cm^2. The theoretical molecular packing density is 0.602 nmol/cm^2 (27.59 $Å^2$). Evidently, F atoms scattering Auger electrons to a lesser extent than carbon and oxygen atoms, based upon measurement of the Auger intensities of the fluorinated aromatics listed in Tables I and II.

(5) Benzyl Mercaptan. The EELS spectrum of benzyl mercaptan (BM), Figure 9, closely resembles the IR spectrum of the solid compound. The EELS spectrum of adsorbed BM differs, as expected, from that of DMBM due to the absence of the O–H stretching band (3500 cm^{-1}), and there are differences in the fingerprint region due to absence of methyl and OH substitutents.

Auger data for BM are given in Table I. Packing densities were obtained by use of eq 26–28 in Table IV. The molecular packing densities, $\Gamma = 0.30$ from Pt signal attenuation and $\Gamma = 0.33$ from carbon Auger signal, were slightly larger than the minimum theoretical limiting value for the orientation where the ring is pendant and parallel to the surface: 0.302 nmol/cm^2 (55.0 $Å^2$). Most efficient packing would be where the ring is rotated perpendicular to the surface; 0.536 nmol/cm^2 (31.0 $Å^2$). Evidently, at this concentration (0.1 mM) BM is adsorbed primarily with the aromatic ring parallel to the surface.

(6) 2,3,5,6-Tetrafluorothiophenol (TFTP2) and 2,3,4,5-Tetrafluorothiophenol (TFTP2). Two other compounds, 2,3,5,6-tetrafluorothiophenol (TFTP4) and 2,3,4,5-tetrafluorothiohenol (TFTP2), provide an opportunity to examine the vibrational spectroscopic differences between ortho and para C–H bands of the vertically oriented adsorbate, Figure 10. Also shown for comparison in the figure are mid-IR spectra of the neat liquids, TFTP2 and TFTP4. In each case there is a striking similarity between the EELS spectrum and the corresponding IR spectrum. In particular, the ortho and para C–H bands in the EELS spectra differ in the same manner as in the IR spectra of the neat liquids.

There is no difference between the EELS spectrum of the adsorbed layer and the IR spectrum of the unadsorbed liquid directly attributable to orientational effects.

Packing densities of TFTP4 were calculated by means of eq 29-32 in Table IV. Packing densities of TFTP2 were calculated from eq 33-35 in Table IV. The results, Tables I and II, resemble those for PFTP. The theoretical packing densities of TFTP4 and TFTP2 are both equal to 0.602 nmol/cm^2 (27.6 Å).

Acknowledgment. This work was supported by the U.S. Department of Energy, Division of Chemical Sciences, Office of Basic Energy Sciences. Instrumentation was provided by the National Science Foundation, Air Force Office of Scientific Research, and the University of Cincinnati.

Spectroscopic Investigations of the Electron Self-Exchange Reaction of the Perchlorate Salt of [1,7-Bis(5-methylimidazol-4-yl)-2,6-dithiaheptane]copper(n+) (n = 1, 2)

C. M. Groeneveld, J. van Rijn, J. Reedijk, and G. W. Canters*

Contribution from the Gorlaeus Laboratories, Leiden University, P.O. Box 9502, 2300 RA Leiden, The Netherlands. *Received September 23, 1987*

Abstract: The electron self-exchange rate of the perchlorate salt of [1,7-bis(5-methylimidazol-4-yl)-2,6-dithiaheptane]copper(n+) (n = 1, 2) in dimethyl sulfoxide has been measured by ^{1}H NMR experiments as a function of temperature between 301 and 355 K. The rate amounts to 4×10^3 M^{-1} s^{-1} at 301 K. A theoretical analysis of the activation parameters, which amount to $\Delta H^* = 9.1$ (0.6) kcal/mol and $\Delta S^* = -11.8$ (1.6) cal/K·mol, shows that the electron-transfer reaction takes place in the adiabatic regime over an electron-transfer distance of 6-7 Å. The dipolar correlation time for the Cu(II) compound amounts to 0.1 ns at 355 K. A Fermi-contact interaction of about 50-100 mG for H2′,2″, H1,5, and Me4′,4″ is compatible with the experimental observations.

Electron self-exchange reactions currently receive considerable attention not only because of their prominent role in the theory of electron transfer but also because they constitute a class of reactions which may provide fundamental insight in the mechanism of electron transfer. Electron self-exchange reactions are inherently simpler to analyze than electron transfer between different redox partners, if only because of the absence of a driving force.

In recent years, a number of studies of electron self-exchange rates of blue-copper proteins have been reported.[1-9] By and large two methods appear applicable to the determination of these rates, first, isotopic labeling (^{63}Cu/^{65}Cu) in combination with rapid flow/freeze techniques[2,4] and, secondly, the NMR study of slightly oxidized solutions of the reduced protein,[1,3,5-9] in cases where the paramagnetic broadening of the NMR signals can be analyzed in the so-called "slow exchange" or "strong-pulse limit".[10,11]

Values of the electron self-exchange rate have been determined experimentally for stellacyanin (1.2×10^5 M^{-1} s^{-1} at 293 K),[2] the azurins from *Pseudomonas aeruginosa* (1.3×10^6 M^{-1} s^{-1} at 309 K)[3] and *Alcaligenes denitrificans* (4×10^5 M^{-1} s^{-1} at 297 K),[6] amicyanin from *Thiobacillus versutus* (8.5×10^4 M^{-1} s^{-1} at 309 K),[9] and plastocyanin from French bean ($k \ll 2 \times 10^4$ M^{-1} s^{-1} at 323 K).[1] There is, therefore, appreciable variation in the electron self-exchange rates of blue-copper proteins, and the high values observed for the azurins have especially intrigued researchers.

Electron self-exchange rates of the blue-copper proteins and the corresponding activation parameters are not readily accessible for a thorough theoretical analysis.[12-15] A study of synthetic and relatively simple model compounds may be helpful and important in this respect. Self-exchange reactions have been studied of the following copper compounds: (tri-α-aminoisobutyric acid)copper(n+) (n = 2, 3) (5.5×10^4 M^{-1} s^{-1} at 298 K),[16] [tetrabenzo[b,f,j,n][1,5,9,13]tetraazacyclohexadecine]copper(n+) (n = 1, 2) (5.5×10^5 M^{-1} s^{-1} at 295 K),[17] bis(1,10-phenanthroline)copper(n+) (n = 1, 2) ($\sim 10^5$ M^{-1} s^{-1}),[18] and (2,6-bis([1-((2-pyridin-2-ylethyl)imino)ethyl])pyridine)copper(n+) (n = 1,2) (1.7×10^3 M^{-1} s^{-1} at 298 K).[19] In addition the self-exchange rates of various complexes have been determined indirectly by the application of the Marcus theory[20] on heterogeneous electron-transfer reactions of these complexes with different redox partners.[21-23] By far the fastest reaction, probably proceeding through

(1) Beattie, J. K.; Fensom, D. J.; Freeman, H. C.; Woodcock, E.; Hill, H. A. O.; Stokes, A. M. *Biochim. Biophys. Acta* **1975**, *405*, 109-114.
(2) Dahlin, S.; Reinhammar, B.; Wilson, M. T. *Biochem. J.* **1984**, *218*, 609-614.
(3) Groeneveld, C. M.; Canters, G. W. *Eur. J. Biochem.* **1985**, *153*, 559-564; *Rev. Port. Quim.* **1985**, *27*, 145.
(4) Groeneveld, C. M.; Dahlin, S.; Reinhammar, B.; Canters, G. W. *J. Am. Chem. Soc.* **1987**, *109*, 3247-3250.
(5) Groeneveld, C. M.; Canters, G. W. *J. Biol. Chem.* **1988**, *263*, 167-173.
(6) Groeneveld, C. M.; Ouwerling, M. C.; Erkelens, C.; Canters, G. W. *J. Mol. Biol.* **1988**, *200*, 189-199.
(7) Groeneveld, C. M.; Dahlin, S.; Reinhammar, B.; Canters, G. W. *Recl. Trav. Chim. Pays-Bas* **1987**, *106*, 279.
(8) Groeneveld, C. M.; Ouwerling, M. C.; Canters, G. W. *Recl. Trav. Chim. Pays-Bas* **1987**, *106*, 280.
(9) Lommen, A.; Canters, G. W. *Recl. Trav. Chim. Pays-Bas* **1987**, 280.
(10) McLaughlin, A. C.; Leigh, J. S., Jr. *J. Magn. Reson.* **1973**, *9*, 296-304.
(11) Canters, G. W.; Hill, H. A. O.; Kitchen, N. A.; Adman, E. T. *J. Magn. Reson.* **1984**, *57*, 1-23.
(12) Sutin, N. *Acc. Chem. Res.* **1982**, *15*, 275-282.
(13) Sutin, N. *Prog. Inorg. Chem.* **1983**, *30*, 442-498.
(14) Marcus, R. A.; Sutin, N. *Biochim. Biophys. Acta* **1985**, *811*, 265-322.
(15) Newton, M. D.; Sutin, N. *Ann. Rev. Phys. Chem.* **1984**, *35*, 437-480.
(16) Koval, K. A.; Margerum, D. W. *Inorg. Chem.* **1981**, *20*, 2311-2318.
(17) Pulliam, E. J.; McMillin, D. R. *Inorg. Chem.* **1984**, *23*, 1172-1175.
(18) Lee, C. W.; Anson, F. C. *Inorg. Chem.* **1984**, *23*, 837-844.
(19) Goodwin, J. A.; Stanbury, D. M.; Wilson, L. J.; Eigenbrot, C. W.; Scheidt, W. R. *J. Am. Chem. Soc.* **1987**, *109*, 2979-2991.
(20) Marcus, R. A. *J. Phys. Chem.* **1963**, *67*, 853-857.
(21) de Korte, J. M.; Owens, G. D.; Margerum, D. W. *Inorg. Chem.* **1979**, *18*, 1538-1542.
(22) Davies, K. M. *Inorg. Chem.* **1983**, *22*, 615-619.
(23) Karlin, K. D.; Yandell, J. K. *Inorg. Chem.* **1984**, *23*, 1184-1188.

0002-7863/88/1510-4893$01.50/0